Correlation between magnetic properties and the electronic structures of soft magnetic ternary $Fe_{78-x}Y_xB_{22}$ (x = 4–9) bulk metallic glasses

2008 J. Phys.: Condens. Matter 20 465105

(http://iopscience.iop.org/0953-8984/20/46/465105)

J. Phys.: Condens. Matter **20** (2008) 465105 (6pp) doi:10.1088/0953-8984/20/46/465105

Correlation between magnetic properties and the electronic structures of soft magnetic ternary $Fe_{78-x}Y_xB_{22}$ ($x = 4$–9) bulk metallic glasses

M T Liu[1], S C Ray[1,7], H M Tsai[1], C W Pao[1], D C Ling[1], W F Pong[1,8], J W Chiou[2], M-H Tsai[3], L Y Jang[4], T W Pi[4], J F Lee[4], C Y Lin[5] and T S Chin[6]

[1] Department of Physics, Tamkang University, Tamsui 251, Taiwan
[2] Department of Applied Physics, National University of Kaohsiung, Kaohsiung 811, Taiwan
[3] Department of Physics, National Sun Yat-Sen University, Kaohsiung 804, Taiwan
[4] National Synchrotron Radiation Research Center, Hsinchu 300, Taiwan
[5] Department of Material Science and Engineering, National Tsing Hua University, Hsinchu 300, Taiwan
[6] Department of Material Science and Engineering, Feng Chia University, Taichung 407, Taiwan

E-mail: wfpong@mail.tku.edu.tw

Received 6 May 2008, in final form 23 September 2008
Published 27 October 2008
Online at stacks.iop.org/JPhysCM/20/465105

Abstract
Fe and Y K-edge extended x-ray absorption fine structure, Fe(Y) $L_{3,2}$-edge (L_3-edge) x-ray absorption near-edge structure (XANES) and valence-band photoemission spectroscopy (VB-PES) measurements have been carried out to study soft magnetic ternary $Fe_{78-x}Y_xB_{22}$ bulk metallic glasses (BMGs). The combined XANES and VB-PES results do not show broadening of the Fe 3d band to support the previous interpretation of the reduction of the magnetic moment in BMGs by Y-induced decrease of exchange splitting of Fe 3d orbitals. Instead, the density of delocalized/itinerant Fe 3d states in the vicinity of the Fermi level is found to be reduced by Y substitution, which reduces the strength of itinerant-states-mediated ferromagnetic coupling between local spins on the Fe ions and the total magnetic moment of the Fe-based BMGs.

(Some figures in this article are in colour only in the electronic version)

1. Introduction

Fe-based bulk metallic glasses (BMGs), which exhibit low saturation magnetization, have attracted considerable attention because of their favorable soft magnetic properties of fundamental interest and industrial exploitability [1–3]. Earlier experimental studies have focused on the evolution of Fe d band hybridization and local atomic order [4, 5], electron transfer between the Fe 3d band and states of nearest neighbors [6], the Fe–Fe coordination number [7] and Fe–Fe nearest-neighbor distances [8], all of which were proposed to be responsible for the various magnetic properties of these Fe-based alloys. Theoretical frameworks of localized and itinerant magnetism [9, 10] have been applied to explain the changes in the magnetic properties of these Fe-based alloys. The former concerns the magnetic moment associated with the local atomic environment [9]. The latter is independent of the local environment but depends closely on the valence state of the metalloid [10]. Calculations based on the first-principles molecular dynamics simulation suggested a dilution effect

[7] Present address: Centre for Advanced Materials, IACS, Jadavpur, Kolkata 700032, India.
[8] Author to whom any correspondence should be addressed. On leave from: Advanced Light Source, LBNL, Berkeley, CA 94720, USA.

by the non-magnetic content in the alloy, which reduces the magnetic moment of the Fe-based alloys [11, 12]. However, the nature of the various magnetic properties of the Fe-based alloys is still debated and not well understood. Recently, Lin *et al* prepared amorphous ternary $Fe_{78-x}Y_xB_{22}$ BMGs by modifying compositional selection rules to enhance the glass forming ability (GFA) of these alloys [13, 14]. A prominent property of $Fe_{78-x}Y_xB_{22}$ BMGs is the decrease of the saturation magnetization with the increase of the Y content. Y has no magnetic moment, it might just simply dilute the magnetization of $Fe_{78-x}Y_xB_{22}$ BMGs. However, since $Fe_{78-x}Y_xB_{22}$ BMGs are amorphous the variation of their magnetic properties is expected to strongly correlate with the local atomic and electronic structures in the alloys, which it was argued should be explained in terms of the short-range effect [4, 5]. Therefore, a microscopic understanding of the local atomic and electronic structures, which provides crucial insight into the magnetic properties of $Fe_{78-x}Y_xB_{22}$ BMGs, is important. Thus, Fe and Y K-edge extended x-ray absorption fine structure (EXAFS), Fe(Y) $L_{3,2}$-edge (L_3-edge) x-ray absorption near-edge structure (XANES) and valence-band photoemission spectroscopy (VB-PES) measurements for $Fe_{78-x}Y_xB_{22}$ BMGs were performed to elucidate the effects of increasing Y content on their magnetic properties.

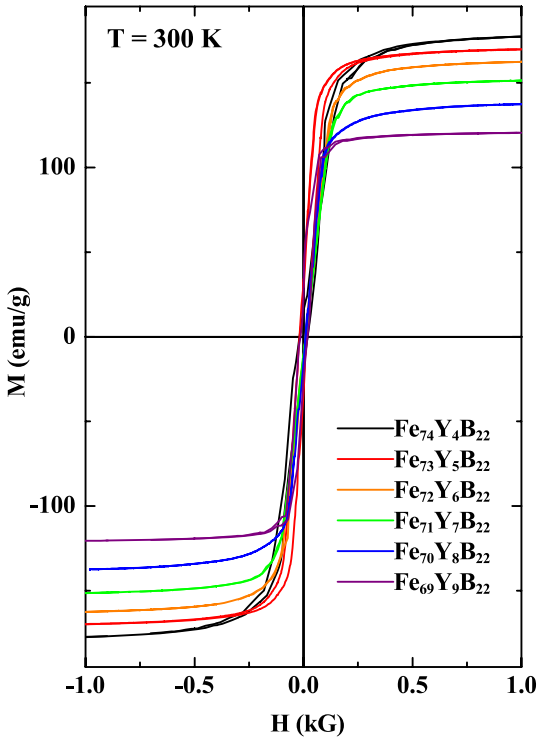

Figure 1. The hysteresis loops of $Fe_{78-x}Y_xB_{22}$ BMGs at room temperature.

2. Experimental details

Fe, Y K-edge EXAFS, Fe(Y) $L_{3,2}$-edge (L_3-edge) XANES and VB-PES spectra were obtained at the National Synchrotron Radiation Research Center, Hsinchu, Taiwan. EXAFS and XANES data were obtained in the fluorescence and sample drain current modes, respectively, while VB-PES spectra were obtained at a photon excitation energy of 110 eV and a base pressure of $\sim 5 \times 10^{-10}$ Torr. The samples were cleaned to eliminate any contaminants, especially oxygen, by Ar^+ bombardment at a very low energy for a very short duration to ensure that the sample films were not damaged. The valence-band spectra were compared before and after the bombardment to make sure that this cleaning procedure did not damage the films and that the oxygen was eliminated. The resolutions were set to 0.2–0.5 eV at a photon energy of 700–2100 eV during XANES measurements, while the resolution of the VB-PES measurement was set to ~0.01 eV. The energy scale was calibrated using the spectra of pure Fe and Y metals. All measurements were performed at room temperature. The XANES spectra shown in the figures have been divided by the incident intensity I_0 and subtracted by the pre-edge background at the L_3-edge. All spectra have been normalized to an edge jump of unity. The normalization procedure was carried out by matching the absorption coefficients from the pre-edge region at L_3-edge to 20 (30) eV above L_2-edge (L_3-edge) for Fe(Y), which is a common practice for the comparison and evaluation of the intensities of resonance absorption spectra of a series of systematically varied compounds [15]. The FT spectra were analyzed by a combination of the multiple-scattering EXAFS computer program FEFF code [16]. The energy of VB-PES has been calibrated by the Fermi energy (E_f) of a clean gold metal. The zero energy refers to the threshold of the emission spectrum and is also referred to as E_f. A series of $Fe_{78-x}Y_xB_{22}$ ($x = 4$–9) ribbons were prepared by the melt-spinning technique. The synthetic method and characterizations of the sample have been detailed elsewhere [13, 14].

3. Results and discussion

Figure 1 displays the magnetization hysteresis loops (M–H curves) of $Fe_{78-x}Y_xB_{22}$ BMGs, which show that amorphous BMGs are ferromagnetic at room temperature and their saturation field decreases as the Y content increases. The saturated magnetic moments of $Fe_{78-x}Y_xB_{22}$ can be estimated from the M–H curves to be ~2.08 μ_B/Fe and 1.53 μ_B/Fe, respectively, for $x = 4$ and 9 in applied magnetic fields up to 0.1 T, which are ~93% and 69% of that of the Fe atom in the *bcc* Fe metal (~2.23 μ_B/Fe) [17], respectively. Apparently, the magnetic moment of $Fe_{78-x}Y_xB_{22}$ decreases monotonically with the increase of x. Figure 2 and the inset present the Fourier transform (FT) amplitude of EXAFS $k^3\chi$ of $Fe_{78-x}Y_xB_{22}$ BMGs and the reference Fe foil and their corresponding oscillation at the Fe K-edge. The general lineshapes, full widths at half-maximum (FWHM) and the radial distribution of the FT spectra for $Fe_{78-x}Y_xB_{22}$ BMGs closely resemble one another, indicating that Fe atoms in $Fe_{78-x}Y_xB_{22}$ BMGs have similar local atomic structures, irrespective of the Y content. The first main peak in the FT curves of $Fe_{78-x}Y_xB_{22}$ can be attributed to the multiple nearest-neighbor (NN) Fe–Fe, Fe–B and Fe–Y bond lengths [5], which shift toward lower radial distance from that

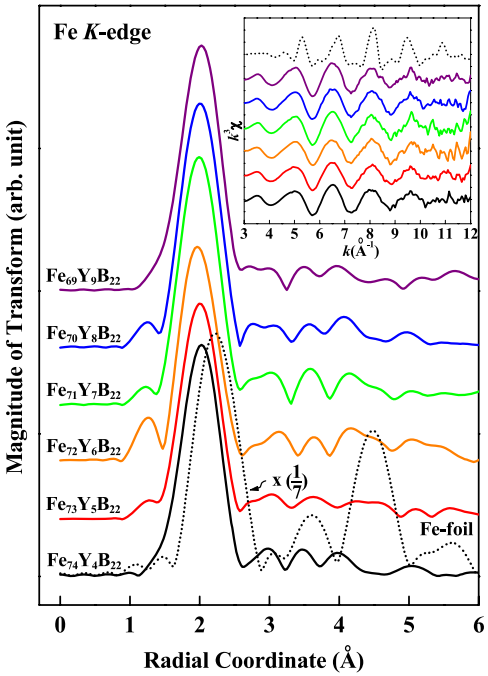

Figure 2. The magnitude of FT of EXAFS $k^3\chi$ at the Fe K-edge of $Fe_{78-x}Y_xB_{22}$ BMGs and the Fe foil (the intensity of the Fe-foil spectra has been scaled by a factor of 1/7) from $k = 3.1$ to 10.6 Å^{-1}. The inset represents the Fe K-edge EXAFS oscillation $k^3\chi$ data.

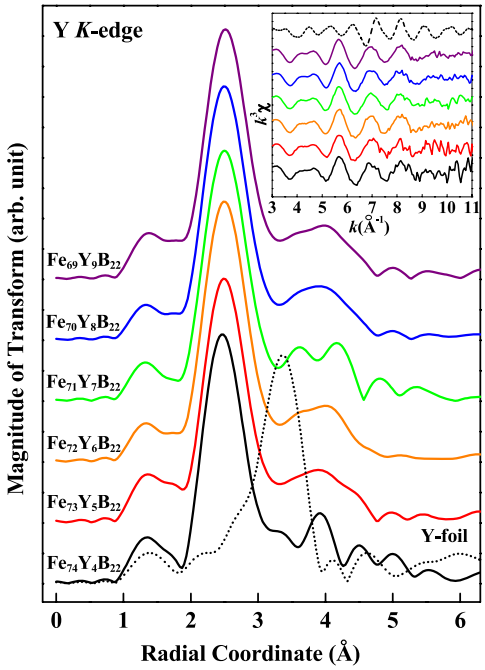

Figure 3. The magnitude of FT of EXAFS $k^3\chi$ at the Y K-edge of $Fe_{78-x}Y_xB_{22}$ BMGs and the Y-foil from $k = 3.0$ to 10.1 Å^{-1} The inset represents the Y K-edge EXAFS oscillation $k^3\chi$ data.

of the Fe foil. Furthermore, the heights of the FT curves of $Fe_{78-x}Y_xB_{22}$ not only are significantly reduced, in particular at a distance larger than ∼3 Å, but also differ substantially from that of the Fe foil, indicating that Fe sites in the $Fe_{78-x}Y_xB_{22}$ BMGs are amorphous. However, the difference in amplitude in the FT EXAFS data of the $Fe_{78-x}Y_xB_{22}$ sample in comparison to the Fe metal foil measured at the Fe K-edge cannot alternatively be interpreted as due to the size effect of nanosized Fe clusters, according to the result of the EXAFS study indicated that the nanosized Fe clusters remain as a bcc structure, the same as Fe metal [18]. In order to understand the details how local atomic structure can affect the magnetic properties of $Fe_{78-x}Y_xB_{22}$ BMGs, the multiple NN bond lengths can be quantitatively evaluated by Fourier analysis of the Mn K-edge EXAFS. However, due to that $Fe_{78-x}Y_xB_{22}$ BMGs are amorphous, the large structural disorder and asymmetry distribution functions for Fe–Fe, Fe–B and Fe–Y pairs [5] complicated the determination of the details of the local atomic environment in $Fe_{78-x}Y_xB_{22}$ BMGs, so that local atomic structures were not presented in this study. However, progressive data analysis is under consideration. Figure 3 and the inset present the FT amplitude of EXAFS $k^3\chi$ of $Fe_{78-x}Y_xB_{22}$ BMGs and the reference Y-foil and their corresponding oscillation at the Y K-edge. In figure 3, the first main peaks in the FT curves of Y K-edge EXAFS $k^3\chi$ is primarily associated with the NN Y–Fe, Y–B and Y–Y bond lengths of $Fe_{78-x}Y_xB_{22}$ [5], which essentially have the same position, suggesting that Y atoms in $Fe_{78-x}Y_xB_{22}$ BMGs have similar local atomic structures and are also insensitive to the Y content. Furthermore, the general lineshapes and radial distribution of the FT spectra for $Fe_{78-x}Y_xB_{22}$ BMGs differ

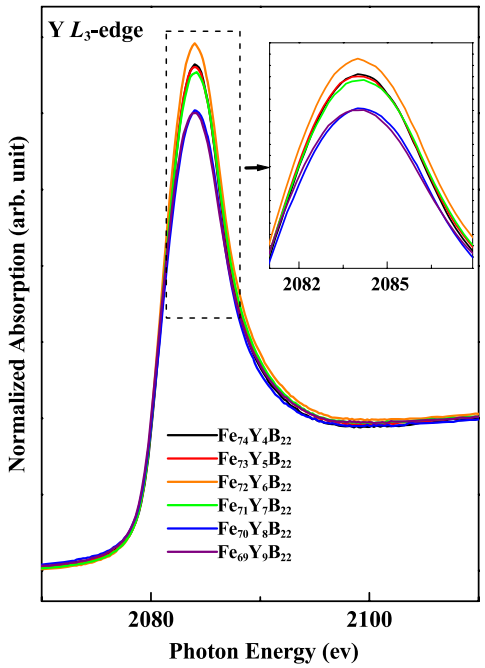

Figure 4. Normalized Y L_3-edge XANES spectra of $Fe_{78-x}Y_xB_{22}$ BMGs. The inset magnified white lines of the Y L_3-edge XANES spectra.

significantly from that of the Y-foil, suggesting that Y sites in the $Fe_{78-x}Y_xB_{22}$ BMGs are also amorphous or a glass network.

Figure 4 displays the normalized Y L_3-edge XANES spectra of $Fe_{78-x}Y_xB_{22}$. The area under the white-line feature in the Y L_3-edge XANES spectra depends not only on the number of 4d holes but also on the dipole-transition probability

from Y $2p_{3/2}$ to the unoccupied Y 4d-derived states, which can be hybridized with Fe d and B p orbitals in the $Fe_{78-x}Y_xB_{22}$ BMGs. The magnified white lines in the inset of the figure show that their intensities do not vary linearly, though overall they decrease as the Y content increases. Why the $Fe_{72}Y_6B_{22}$ ($x = 6$) sample yields the largest intensity at the Y L_3-edge XANES is unclear, which may be related to the experimental finding that $Fe_{72}Y_6B_{22}$ ($x = 6$) has the best GFA among BMGs with soft magnetic properties [13, 14]. In the case of metallic alloys, one could expect the intensities of white-line features to depend on the charge transfer of constituent ions and the charge count within the atomic Winger–Seitz volume, which tends to remain neutral [19]. However, charge neutrality is a general rule over the Winger–Seitz volume, which includes space shared by surrounding ions. Charge redistribution of localized d electrons and itinerant sp conduction electrons according to the relative electronegativity of the constituent ions also affects the various intensities of white lines at the Y L_3-edge in the $Fe_{78-x}Y_xB_{22}$ BMGs.

Figure 5 displays the normalized Fe $L_{3,2}$-edge XANES spectra of $Fe_{78-x}Y_xB_{22}$ BMGs and Fe foil. According to the dipole-transition selection rule, the dominant transition is from Fe $2p_{3/2}$ and $2p_{1/2}$ to the unoccupied Fe 3d states. The area under the white-line feature in the Fe $L_{3,2}$-edge XANES spectrum is predominately a convolution of the absolute square of the transition matrix element and the unoccupied density of states (DOSs) of the Fe 3d electrons. The general lineshapes in the Fe $L_{3,2}$-edge XANES spectra of $Fe_{78-x}Y_xB_{22}$ BMGs have similar features, except for the intensities near the threshold. The inset of figure 5 reveals a decrease in the intensity of the white-line feature at the Fe L_3-edge with increasing Y content, after the background intensity described by an arctangent function, indicated by the dashed line in figure 5, is subtracted. In principle, the lower the intensity of the white-line feature in the Fe L_3-edge XANES spectrum, the smaller is the density of the unoccupied Fe 3d states, which would imply an enhancement of Fe 3d-orbital occupation induced by Y substitution. However, the VB-PES measurements to be described later show a decrease of the density of occupied valence states in the vicinity of E_f with the increase of Y content, which seems to suggest a decrease rather than an increase of the overall density of occupied Fe 3d states. This puzzle can be clarified by noting that $Fe_{78-x}Y_xB_{22}$ alloys are metallic, so that their valence states are expected to include Fe 3sp and Y 5sp states, although Fe 3d and Y 4d contribute predominantly to the DOSs in the vicinity of E_f. Thus, Y-induced slight reduction of the intensity of the VB-PES spectra may not necessarily be due to a decrease of the density of occupied Fe 3d states. Nevertheless, the enhancement of Fe 3d occupation does not necessarily mean an enhancement of magnetic moment, which would be opposite to the trend observed in the hysteresis loop measurements, as shown in figure 1, because magnetic moment depends on the spin polarization, not the total number of 3d electrons. Becker and Hafner [12] and Ching *et al* [20] argued that Y-induced enhancement of Fe 3d–Y 4d hybridization reduces exchange splitting of majority-spin (↑-spin) and minority-spin (↓-spin) states, which then reduces the magnetic moment in the Fe–Y

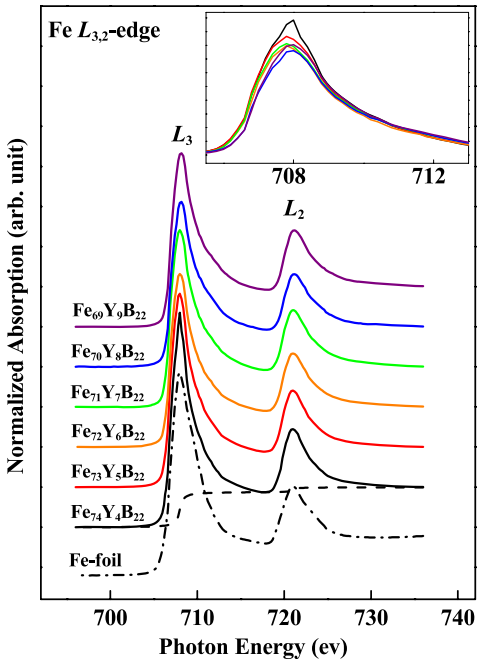

Figure 5. Normalized Fe $L_{3,2}$-edge XANES spectra of $Fe_{78-x}Y_xB_{22}$ BMGs and Fe foil. The inset shows Fe L_3-edge XANES spectra after subtraction using an arctangent function shown in the spectra, indicating a decrease of the intensity with the increase of the Y content in the alloys.

alloys. However, Fe 3d–Y 4d or Fe 3d–Y 5sp hybridization is expected to broaden the Fe 3d band, which is not supported by the trend of the Fe L_3-edge XANES spectra shown in the inset of figure 5. This inset shows that FWHM of the white-line feature does not increase with the increase in Y content. Instead, FWHM decreases slightly with the increase in Y content. In the case of the Y L_3-edge of $Fe_{78-x}Y_xB_{22}$, the FWHM increases from 7.4 (for $x = 4$) to 8.2 eV (for $x = 9$) and the peak intensity decreases gradually from $x = 4$ to 9 for the peak at ∼2084 eV. However, $Fe_{72}Y_6B_{22}$ ($x = 6$) is exceptional and shows the largest intensity, which may be due to the formation of the best GFA among the series of BMGs with soft magnetic properties [13, 14]. In the case of the Fe L_3-edge of $Fe_{78-x}Y_xB_{22}$, the FWHM also increases from 2.2 (for $x = 4$) to 2.6 eV (for $x = 7$) and remains unchanged up to $x = 9$ and the peak intensity decreases from $x = 4$ to 9 for the peak at ∼708 eV, which indicate hybridization between Fe 3d–Y 4d/5sp. The FWHM at the Fe L_3-edge does not increase beyond $x = 7$ in the BMG series and is regarded as a saturation effect.

Thole and van der Laan [21] noted that the branching ratio of the white-line intensity, $I(L_3)/[I(L_3) + I(L_2)]$, depends on the electrostatic interaction between the core–hole and valence electrons (final-state effect) and the initial-state spin–orbit splitting in 3d transition-metal ions and the spin states of the 3d transition-metal ions. It has been established that a larger branching ratio is generally associated with a larger number of unoccupied 3d-derived states and a higher-spin state of amorphous Fe-based alloys [22]. In the present case, the branching ratio is reduced from ∼0.69 ($x = 4$) to 0.65

($x = 9$) at the Fe $L_{3,2}$-edge spectra for $Fe_{78-x}Y_xB_{22}$ BMGs, as presented in figure 6. The intensities of $I(L_3)$ and $I(L_2)$ are the integrated areas in the range of 702–718 eV (for the L_3-edge) and 718–736 eV (for the L_2-edge), respectively, after the respective spectrum is subtracted using an arctangent function as indicated by the dashed line in figure 5. The branching ratio $I(L_3)/[I(L_3) + I(L_2)]$ in the Fe $L_{3,2}$-edge spectra decreases as the Y content increases, illustrating that the spin moments of the electrons in the Fe 3d states are systematically reduced as the Y content increases. This result is consistent with the general trend of the magnetic moment per Fe atom in the $Fe_{78-x}Y_xB_{22}$ BMGs, plotted with red solid circles in figure 6, deduced from M–H curves presented in figure 1.

The inset in figure 6 displays the VB-PES spectra of $Fe_{78-x}Y_xB_{22}$ ($x = 4$, 6 and 8) obtained using an incident photon energy of 110 eV. As the cross section of B 2sp states is much smaller than those of Fe 3d and Y 4d states at 110 eV [23], the intensities of the features in the vicinity of the E_f in the VB-PES spectra presented in the inset of figure 6 are primarily yielded by occupied Fe 3d and Y 4d states. The spectra exhibit a distinctive sharp E_f cutoff, certifying that these alloys are metallic. The spectra have three prominent features, marked by ***a*** (at ∼0.3 eV), ***b*** (∼1.5 eV) and ***c*** (∼5.0 eV), which were assigned by Xu *et al* to be associated with the DOSs of Fe $3de_g$, t_{2g} and Y 4d states [24], respectively. The region in the VB-PES spectra between 3 eV and E_f is enlarged in the inset of figure 6, which shows that features ***a*** and ***b*** of the $x = 8$ sample have a markedly lower spectral intensity than those of $x = 6$ and 4 samples. This trend suggests a decrease of the overall density of occupied Fe 3d states in the vicinity of E_f.

The magnetic moment of a transition-metal ion results from the first Hund's rule or Pauli exclusion principle, which tends to line up spins of valence or open-shell d electrons in the ion to maximize the (negative) total exchange energy. Delocalization of part of the valence d orbitals in metals due to the formation of metallic bonding reduces the magnitude of the exchange energy between two d orbitals and the total spin magnetic moment. That is why Fe metal has a magnetic moment per Fe atom of ∼2.23 μ_B/Fe, in contrast to 4.0 μ_B/Fe of a *free* Fe atom. Ferromagnetism results from alignment of local spins mediated by spin-polarized near-E_f itinerant electrons or states through favorable exchange interactions between these itinerant (or conduction) electrons and local spins. In these BMGs, the total magnetic moment is composed of the magnetic moment of the local spin, d orbitals and spin-polarized itinerant electrons. The decrease of the magnetic moment observed by magnetic hysteresis loop measurements in relationship with the general trend of the decrease of density of Fe 3d states in the vicinity of E_f with the increase of Y content as observed by XANES and VB-PES measurements can be understood in the following. Y can affect the magnetic property of $Fe_{78-x}Y_xB_{22}$ in two ways. One is that substitution of Fe by Y ions reduces the concentration of Fe ions or local spins and increases the average distance between neighboring spins. For the so-called itinerant ferromagnetic material like $Fe_{78-x}Y_xB_{22}$, which is confirmed by the sharp cutoff of VB-PES spectra shown in the inset of figure 6, the ferromagnetic coupling between spins is via itinerant states in the vicinity of E_f. Another is that Y has a Pauling electronegativity (1.22) much smaller than that of Fe and B (1.83 and 2.04, respectively) [25], so that substitution of Fe ions by Y ions increases (reduces) significantly the ionic (metallic) character of the materials, which is equivalent to the reduction of the total density of itinerant states in the vicinity of E_f and reduces not only the strength of ferromagnetic couplings between the spins of Fe ions, but also the contribution of the magnetic moment associated with spin-polarized itinerant electrons.

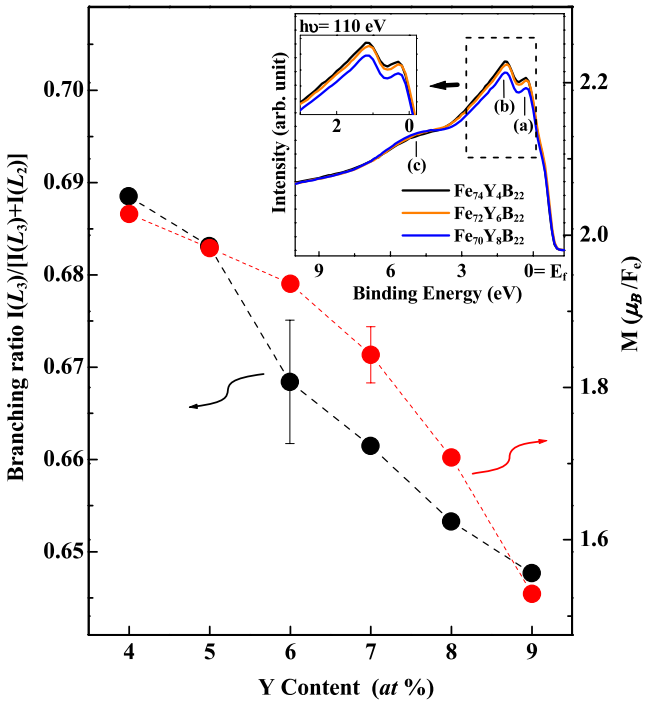

Figure 6. Branching ratio $I(L_3)/[I(L_3) + I(L_2)]$ at the Fe $L_{3,2}$-edge and the magnetic moment obtained from the magnetization hysteresis loop measurements (in figure 1) as a function of the Y content. The inset presents VB-PES spectra of $Fe_{78-x}Y_xB_{22}$ ($x = 4$, 6 and 8) BMGs.

4. Conclusions

In summary, this work investigated the atomic and electronic structures of the amorphous $Fe_{78-x}Y_xB_{22}$ BMGs using x-ray absorption and VB-PES. A combination of the Fe $L_{3,2}$-edge XANES and VB-PES results show that the substitution of Fe ions by Y ions does not broaden the Fe 3d band, which does not support the previous interpretation of the decrease of the magnetic moments in these BMGs caused by the reduction of the exchange splitting of Fe 3d orbitals arising from Fe 3d–Y 4d hybridization. Based on the observed XANES and VB-PES results, the decrease of the magnetic moment induced by the Y substitution can be understood as a reduction of the density of delocalized/itinerant states in the vicinity of E_f. As a result, it weakens the strength of the ferromagnetic coupling between Fe 3d local spins mediated by these itinerant states and the magnetic moment associated with the spin-polarized itinerant electrons.

Acknowledgments

The authors (DCL and WFP) would like to thank the National Science Council of Taiwan for financially supporting this research under contract nos. NSC96-2112-M032-008-MY3 and NSC96-2112-M032-012-MY3.

References

[1] DeCristofaro N 1998 *MRS Bull.* **23** 50
[2] Shen B, Chang C, Zhang Z and Inoue A 2007 *J. Appl. Phys.* **102** 023515
[3] Yao K F and Zhang C Q 2007 *Appl. Phys. Lett.* **90** 061901
[4] Morrison T I, Brodsky M B, Zaluzec N J and Sill L R 1985 *Phys. Rev.* B **32** 3107
[5] Morrison T I, Foiles C L, Pease D M and Zaluzec N J 1987 *Phys. Rev.* B **36** 3739
[6] García-Arribas A, Fdez-Gubieda M L, Orúe I, Barandiarán J M, Herreros J and Plazaola F 1995 *Phys. Rev.* B **52** 12805
[7] Hasegawa R and Ray R 1978 *J. Appl. Phys.* **49** 4174
[8] Fdez-Gubieda M L, García-Arribas A, Barandiarán J M, López Antón R, Orue I, Gorria P, Pizzini S and Fontaine A 2000 *Phys. Rev.* B **62** 5746
[9] Corb B W, O'Handley R C and Grant N J 1983 *Phys. Rev.* B **27** 636
[10] Malozemoff A P, Williams A R and Moruzzi V L 1984 *Phys. Rev.* B **29** 1620
[11] Hafner J, Tegze M and Becker Ch 1994 *Phys. Rev.* B **49** 285
[12] Becker Ch and Hafner J 1994 *Phys. Rev.* B **50** 3913
[13] Lin C Y, Tien H Y and Chin T S 2005 *Appl. Phys. Lett.* **86** 162501
[14] Lin C Y and Chin T S 2007 *J. Alloys Compounds* **437** 191
[15] Heald S M 1988 *X-ray Absorption: Principle, Applications, Techniques of EXAFS, SEXAFS, and XANES* ed D C Koningsberger and R Prins (New York: Wiley)
[16] Ankudinov A L, Ravel B, Rehr J J and Conradson S D 1998 *Phys. Rev.* B **58** 7565
[17] Stöhr J and Siegmann H C 2006 *Magnetism, from Fundamentals to Nanoscale Dynamics* (Berlin: Springer)
[18] Baker S H, Roy M, Louch S and Binns C 2006 *J. Phys.: Condens. Matter* **18** 2385
[19] Hsieh H H, Chang Y K, Pong W F, Pieh J Y, Tseng P K, Sham T K, Coulthard I, Naftel S J, Lee J F, Chung S C and Tsang K L 1998 *Phys. Rev.* B **57** 15204
[20] Ching W Y, Xu Y N, Harmon B N, Ye J and Leung T C 1990 *Phys. Rev.* B **42** 4460
[21] Thole B T and van der Laan G 1988 *Phys. Rev.* B **38** 3158
[22] Cheng Y H, Jan J C, Chiou J W, Pong W F, Tsai M-H, Hsieh H H, Chang Y K, Dann T E, Chien F Z, Tseng P K, Leu M S and Chin T S 2000 *Appl. Phys. Lett.* **77** 115
[23] Yeh J J and Lindau I 1985 *At. Data Nucl. Data Tables* **32** 1
[24] Xu Y B, Greig D, Seddon E A and Matthew J A D 1997 *Phys. Rev.* B **55** 11442
[25] *Table of Periodic Properties of the Elements* 1980 (Skokie, IL: Sargent-Welch Scientific Company)